Article

Reduction and Immobilization of Movable Cu^{2+} Ions in Soils by Fe$_{78}$Si$_9$B$_{13}$ Amorphous Alloy

Liefei Pei, Xiangyun Zhang and Zizhou Yuan *

School of Materials Science and Engineering, Lanzhou University of Technology, Lanzhou 730050, China;
plf0810@hotmail.com (L.P.); LZ2862980790@hotmail.com (X.Z.)
* Correspondence: yuanzz@lut.edu.cn; Tel.: +86-18893816081

Abstract: The Fe-based amorphous alloy (Fe$_{78}$Si$_9$B$_{13}$^{AP}) is applied to the remediation of copper contaminated soil for the first time. The dynamic process of conversion of movable Cu to immobilized forms in the soil system is analyzed. In addition, the dynamic process of form transformation of Cu^{2+} ions in the soil system is analyzed. The morphology and phase composition of the reaction products are characterized by scanning electron microscopy (SEM) and X-ray diffraction analysis (XRD). Finally, the feasibility of recovering residual stabilizer particles and attached immobilized copper by the magnetic separation process is discussed. The results show that the apparent reaction rate constant of Fe$_{79}$Si$_9$B$_{13}$^{AP} with Cu^{2+} ions is higher than that of zero valent iron (ZVI) at all the experimental temperatures. According to the Arrhenius formula, the apparent activation energy of the reaction of Fe$_{78}$Si$_9$B$_{13}$^{AP} and ZVI with Cu^{2+} ions is 13.24 and 19.02 kJ/mol, respectively, which is controlled by the diffusion process. The lower apparent activation energy is one of the important reasons for the high reaction activity of Fe$_{78}$Si$_9$B$_{13}$^{AP}. After 7 days of reaction, a continuous extraction of the experimental soil shows that the main form of copper in the immobilized soil is Cu and copper combined with iron (hydroxide) oxide, and there is almost no soluble copper with a strong mobility, which effectively reduced the bioavailability of copper in the soil. The magnetic separation results of the treated soil show that the recovery rates of immobilized copper in Fe$_{78}$Si$_9$B$_{13}$^{AP} and soil are 47.23% and 21.56%, respectively, which reduced the content of iron and copper in the soil to a certain extent. The above experimental results show that Fe$_{78}$Si$_9$B$_{13}$^{AP} is a promising new material for the remediation of heavy metal contaminated soils, and provides more new references for the application of amorphous alloys in the field of remediation of water and soil contaminated by heavy metals and organic matter.

Keywords: amorphous alloy; soil contamination; heavy metal; magnetic separation

1. Introduction

Soil heavy metal pollution has a large base and strong mobility, which has become an important factor restricting national sustainable development and endangering human health. Copper is one of the essential trace elements for the human body, but the high content of copper has adverse effects on animals, plants, and the human body. Baryla et al. [1] found that excessive copper can cause the concentration difference between the two sides of the plasma membrane, resulting in the flow of potassium ions out of the cell membrane, thus damaging the plasma membrane of plant roots. Dijendra et al. [2] reported that when mice were fed with a diet containing copper (15 mg/kg), their liver morphology and function would show symptoms of poisoning, and the decrease of superoxide dismutase activity would lead to mitochondrial dysfunction, and eventually lead to the death of hepatocytes. Choudhary et al. [3] reported that under the stress of heavy metals such as Cu, the growth of cyanobacteria is inhibited by the increase in the amount of proline, malondialdehyde, and superoxide dismutase. The main source of copper pollution is exogenous copper, such as waste water discharged from mining and the storage of waste

ore. These open-pit wastes continue to diffuse into the surrounding soil under the effects of weathering, acidification and rainfall, resulting in copper substances that enter the soil [4,5]. Water-soluble and exchangeable copper has good solubility and mobility, which can enter the plant through the root of the plant, affecting the normal metabolic activity of the plant [6–8]. From the point of view of ecological risk assessment, it is valuable to transform movable Cu^{2+} ions into an immobilized state with low bioavailability [9]. In recent years, researchers have developed a series of soil stabilizers for immobilization remediation of heavy metal contaminated soils. For example, Zhang et al. [10] studied the immobilization performance and mechanism of novel phosphorus-modified biochars on soil heavy metals. The experimental results show that by forming precipitates or complexes with Cu^{2+} ions, the phosphorus compounds in surface modified biochar can reduce the leaching amount of Cu^{2+} ions by 2–3 times and promote the conversion of Cu^{2+} ions from an acid solution to a stable state. Viglašová E. et al. [11] studied the adsorption process of Cu^{2+} by natural bentonite, Illite, and montmorillonite under different experimental conditions. The results show that the adsorption is realized by the ion exchange process, achieving a balance within 15 min. The adsorption capacity of the three materials for Cu^{2+} is bentonite 0.0658 mg/g, Illite 0.0663 mg/g, and montmorillonite 0.0667 mg/g, respectively. Cui et al. [12] remediated copper contaminated soil by adding 1–5% hematite to hydroxyapatite as a soil stabilizer. After 42 days of the flooding culture experiment, the soil redox potential decreases, pH increases, and extractable copper decreases by 53.7%. The immobilization process did not cause a secondary pollution to the environment. Therefore, immobilization is an efficient and economical method for soil remediation.

Among the many chemical immobilization methods, it is one of the most commonly used methods to immobilize heavy metal ions by the redox process, and then adsorb them to their corrosion products by gluing or precipitation [13,14]. Soil stabilizers should be reasonably selected according to different types of pollutants in soil immobilization remediation. Copper has a high electrode potential ($Z(Cu^{2+}/Cu^0)$ = +0.34 V). It is an effective method to convert movable Cu^{2+} ions into immobilized copper by the redox reaction. Zero-valent iron (ZVI) is a low-cost environment-friendly reductant ($Z(Fe^{2+}/Fe^0)$ = −0.44V), which is widely used in the degradation of environmental pollutants [15–17]. Frick et al. [18] remediation of chromated copper arsenates (CCA) contaminated soil with the ZVI-biochar combined stabilizer reduced the contents of water-soluble Cr, Cu, and As by 45%, 45%, and 43%, respectively. However, the treatment effect of using ZVI or biochar alone is not ideal. The main reason is that the adhesion of the reaction products to the surface of ZVI hinders the contact between Cu^{2+} ions and fresh ZVI surface, thus blocking the progress of the reaction. Kumpiene et al. [19] used ZVI to reduce the mobility and bioavailability of copper and arsenic in soils. The content of As^{5+} ions decrease by 99%, but the content of Cu^{2+} ions in the soil is still high, which has a certain residual toxicity to the soil. It can be seen that the immobilization effect of traditional stabilizers on Cu contaminated soil is not ideal. Therefore, there is an urgent need to develop new stabilizers with excellent performance and low cost in the field of soil remediation.

Amorphous alloy (MGs) is a thermodynamic metastable alloy formed by rapid solidification of molten metal at a cooling rate of more than 379 K/s [20]. The atomic arrangement of its components is far from the equilibrium position, showing the characteristics of long-range disorder and short-range order. This unique stacking structure of disordered atoms determines that it has excellent properties incomparable to crystalline alloys [21,22]. In 2010, Zhang et al. [23] used the Fe-Mo-Si-B amorphous alloy to degrade direct blue 2B for the first time. The results show that the reaction rate of direct blue 2B degradation of the Fe-Mo-Si-B amorphous alloy is four times higher than that of the same component crystalline alloy. This opens the research on the application of MGs in the field of environmental pollutant degradation. Zhang et al. [24] compared the reduction and removal ability of Cu^{2+} ions between $Fe_{79}Si_{13}B_8{}^{AR}$ and 300 mesh iron powder. The results show that the normalization rate constant of the $Fe_{79}Si_{13}B_8{}^{AR}$ surface area is 167 times higher than that of the 300 mesh iron powder. Liang et al. [25] used $Fe_{79}Si_{13}B_8{}^{AR}/Na_2S$ to remove

As^{5+} from the groundwater. As^{5+} is reduced to As^{3+} by $Fe_{79}Si_{13}B_8{}^{AR}$ and then combined with S^{2-} to form the As_2S_3 precipitation. The removal rate of As^{5+} is more than 95% after 60 min. Some scholars attribute the high reactivity of MGs to the fact that the metastable structure of disordered arrangement of atoms makes the surface diffusion rate of MGs millions of times higher than that of the bulk phase [26,27].

Inspired by the previous research results, the $Fe_{79}Si_{13}B_8{}^{AP}$ is applied to the immobilization and remediation of copper contaminated soil for the first time in this paper. The kinetic process of conversion of movable Cu to immobilized forms in soil and the effect of product morphology on the reaction rate are studied. Then, the feasibility of recovering residual $Fe_{79}Si_{13}B_8{}^{AP}$ particles and copper immobilized on their surfaces by the magnetic separation process is explored. Providing more new references for the application of MGs in the field of environmental pollutant degradation is expected.

2. Materials and Methods

2.1. Materials

The reagents used in this experiment include $CuSO_4 \cdot 5H_2O$, HCl, NaOH, $MgCl_2$, HNO_3, CH_3COONH_4, CH_3COOH, $NH_4OH \cdot HCl$, and H_2O_2. These reagents were purchased from Lanzhou Moer Chemical Products Co. Ltd. (Lanzhou, China). ZVI powders were purchased from China Zhongye Chemicals Co. Ltd. (Xingtai, Hebei, China), which have a mean grain size (d_{50}) of ~1 μm. The price of the powders is CNY 740/kg. $Fe_{78}Si_9B_{13}{}^{AP}$ with an average particle size of 10 μm were purchased from Beijing Yijin Chemicals Co. Ltd. (Beijing China). The price is CNY 770/kg.

2.1.1. Soil Sample Collection

Surface loess soil without copper contamination was collected from Lanzhou suburb of Gansu Province (36°03′ N, 103°49′ E) and sifted through a 2 mm sieve. After screening, it was washed with distilled water three times to remove soluble compounds and suspended particles. The washed soil was air-dried and then passed through the 2 mm sieve again, and the obtained soil was put into a sample bag for backup.

2.1.2. Preparation of Contaminated Soil

The soil environmental quality standard of the People's Republic of China stipulates that the upper limit of copper contaminated soil is 200 mg/kg [28]. In addition, the maximum content of copper in the soil around the Baiyin copper smelter, known as "Copper City of China", is 658 mg/kg [29]. As a result, the content of copper in the contaminated soil was determined to be 600 mg/kg. The specific steps were as follows: Mixing a 1 L $CuSO_4 \cdot 5H_2O$ solution of 60 mg/L with 100 g washed soil and then mechanically stirring until air-dried. In order to determine the uniformity of Cu in soil when different volumes of water were added to soil samples of the same quality. The concentration of Cu^{2+} ions were inversely proportional to the volume of distilled water, indicating that Cu has been uniformly dispersed in the soil.

2.2. Immobilization of Cu^{2+} Ions in the Soil: Batch Test

The immobilization effect of $Fe_{79}Si_{13}B_8{}^{AP}$ and ZVI on Cu^{2+} ions in the soil was evaluated under the experimental temperature of 293, 303, 313, and 323 K. In order to remove the surface oxide layer as much as possible, the stabilizer was leached with 2% HNO_3 before each batch of test. Each group of experiments was carried out in a series of 100 mL jars, and the preparation of slurry in each jar was as follows: 5 g of copper contaminated soil was mixed with 50 mL deionized water, then shaken in a water bath shaker for 5 min to completely wet the soil to form a soil suspension. According to the method of Shaaban et al. [30], the initial pH of the reaction system was adjusted to 6 by HCl and NaOH. In general, increasing the amount of stabilizer is beneficial to the immobilization of heavy metal ions [31]. However, when the content of iron in the soil is more than 5%, it will inhibit the growth of plants [32]. As a result, the dosage of

$Fe_{78}Si_9B_{13}{}^{AP}$ and ZVI was selected as 5% of the soil mass, that is, 0.25 g was added to the jar. When the soil reacted for 1, 2, 4, 8, 16, 24, 36, and 48 h, it was continuously extracted according to the method of Ure et al. [33]. The content of Cu^{2+} ions in each extract was determined by inductively coupled plasma atomic emission spectrometry (ICP-AES). After the remaining two slurries continued to react for 7 days, one of them was continuously extracted according to the above-mentioned method. The other slurry carried out magnetic separation of the treated soil according to the method described by Guan [34] to separate the immobilized products and stabilizer particles. Table 1 shows all the reagents of the continuous extraction method.

Table 1. Continuous extraction of metals in the soil.

Index	Speciation	Extraction Agents and Conditions
SE	soluble and exchangeable	0.01 mol/L $MgCl_2$, 50 mL; 0.11 mol/L acetic acid (CH_3COOH), 20 mL
OX	reducible state	0.5 mol/L $NH_4OH \cdot HCl$, 20 mL
OM	oxidizable state	Hydrogen peroxide (H_2O_2) at 85 °C and 1 mol/Lammonium acetate (CH_3COONH_4)
RE	residual	Aquaregia (HCl:HNO_3, 1:3 *v/v*), 160 °C

In order to accurately analyze the copper in the immobilization reaction and the rate control process of the reaction of $Fe_{78}Si_9B_{13}{}^{AP}$ and ZVI with Cu^{2+} ions in soil. The experimental results were fitted by the pseudo-first-order kinetic Equation (1) linear fitting:

$$C_t/C_0 = \exp(-k_{obs}t) \tag{1}$$

where t is the reaction time (h); C_t is the concentration of SE at the current time (mg/kg); C_0 is the concentration of SE at the initial time (mg/kg); and k_{obs} is the observed pseudo-first-order reaction rate constant.

The reaction activation energy (ΔE) is an important parameter to characterize the kinetic process of the chemical reaction. ΔE can be obtained according to the Arrhenius-type equation (Equation (2)):

$$\ln k_T = -\Delta E/RT + \ln A \tag{2}$$

where k_T is the k_{obs} obtained by Equation (1) at different temperatures. R is the gas constant, $R = 8.314$ J/(mol·K); A is the constant.

2.3. Characterization Techniques

The surface morphology changes of $Fe_{78}Si_9B_{13}{}^{AP}$ and ZVI before and after the reaction were observed by the scanning electron microscope (SEM, JSM-6700, JEOL, Akishima, Japan). The structural characterizations of the stabilizer and the composition of the reaction product were identified by X-ray diffraction (XRD, D8 ADVANCE, BRUKER, Karlsruhe, Germany) with Cu-Kα radiation (40 kV, 150 mA).

3. Results and Discussion

3.1. Characterization of $Fe_{78}Si_9B_{13}{}^{AP}$ and ZVI

Figure 1 shows the structural and morphological differences between $Fe_{79}Si_{13}B_8{}^{AP}$ and ZVI before the soil remediation experiments. In Figure 1a, the crystalline α-Fe phase is observed in the X-ray diffraction spectrum of ZVI, and there is no crystallization peak of iron oxide, indicating that the purity of ZVI is high and the surface is not oxidized. There is a diffuse scattering peak in the X-ray diffraction spectrum of $Fe_{79}Si_{13}B_8{}^{AP}$ around 45°, and there is no crystallization peak in the rest of the X-ray diffraction spectrum, indicating that it is amorphous. Since there are no lattice fringes and lattice diffraction spots in the TEM and SAED images in Figure 1b, this conclusion is further confirmed. Figure 1c,d shows the SEM images of $Fe_{79}Si_{13}B_8{}^{AP}$ and ZVI, respectively. The two kinds of powders have a spherical structure with a smooth surface and there is no adhesion between the particles. The particle size of $Fe_{78}Si_9B_{13}{}^{AP}$ is 10–20 μm, and that of ZVI is 1–3 μm.
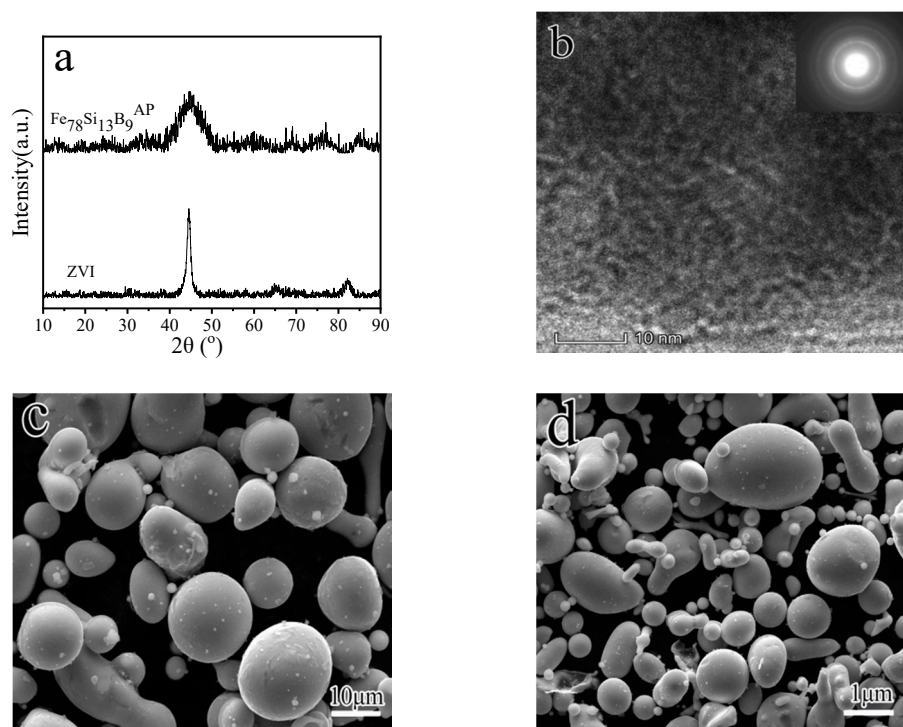
Figure 1. XRD spectra and SEM of the iron-based materials: (**a**) The XRD patterns; (**b**) the TEM image of $Fe_{78}Si_9B_{13}{}^{AP}$; (**c**) the surface morphology of $Fe_{78}Si_9B_{13}{}^{AP}$; (**d**) the surface morphology of zero valent iron (ZVI).

3.2. Cu^{2+} immobilization by $Fe_{78}Si_9B_{13}{}^{AP}$ and ZVI

Figure 2a,b shows the exponential decay curve of the normalized concentration of Cu^{2+} reacting with $Fe_{78}Si_9B_{13}{}^{AP}$ and ZVI at different temperatures. The reaction of each experimental group basically ended within 10 h, and there is no secondary dissolution after 10 h, indicating that the reduction products could stably exist in the reaction system. Figure 2c shows the k_{obs} obtained by fitting the quasi-first-order kinetic equation (Equation (1)). With the increase of the reaction temperature from 293 to 323 K, the k_{obs} of each experimental group shows an upward trend. The k_{obs} of $Fe_{78}Si_9B_{13}{}^{AP}$ increases from 0.955 to 1.568 h^{-1}. The k_{obs} of ZVI is significantly lower than that of $Fe_{78}Si_9B_{13}{}^{AP}$. Generally speaking, the smaller the particle size and the higher the content of the reactant, the more conducive it is to speeding up the reaction [35,36]. However, in this experiment, the k_{obs} of ZVI with a relatively small particle size and higher iron content reacting with Cu^{2+} are lower than $Fe_{78}Si_9B_{13}{}^{AP}$ with a relatively large particle size and lower iron content, which may be due to the metastable state of MGs caused by the structure.

As we all know, the activation energy (ΔE) reflects an important kinetic parameter of the difficulty of the chemical reaction [37]. On the basis of the above k_{obs}, the ΔE difference between crystalline and amorphous iron-based materials is further analyzed. The illustrations in Figure 2a,b are shown as straight lines fitted by the Arrhenius-type equation (Equation (2)) for the k_{obs} which was reacted by $Fe_{78}Si_9B_{13}{}^{AP}$ and ZVI with Cu^{2+} at different temperatures. The correlation coefficients R^2 are all above 0.99. The ΔE of $Fe_{78}Si_9B_{13}{}^{AP}$ is 13.24 kJ/mol, while the ΔE of ZVI which is significantly higher than that of $Fe_{78}Si_9B_{13}{}^{AP}$ is 19.02 kJ/mol. In other words, $Fe_{78}Si_9B_{13}{}^{AP}$ needs less energy to transform from a normal state to an active state where chemical reactions easily occur. This is due to the higher Gibbs free energy of MGs than crystalline alloys [38]. It also explains why the k_{obs} of $Fe_{78}Si_9B_{13}{}^{AP}$ is higher than that of ZVI. The ΔE of the general chemical reaction is between 60–250 kJ/mol. The ΔE of the reaction between iron-based materials and Cu^{2+} is lower than that of 60 kJ/mol [39]. According to the diffusion theory, when ΔE is within the range of 8–22 kJ/mol, the reaction is controlled by an external diffusion [40]. The ΔE of

the two materials is in this range, indicating that the adsorption of soil to Cu^{2+} hinders the effective contact between Cu^{2+} and the reaction surface.
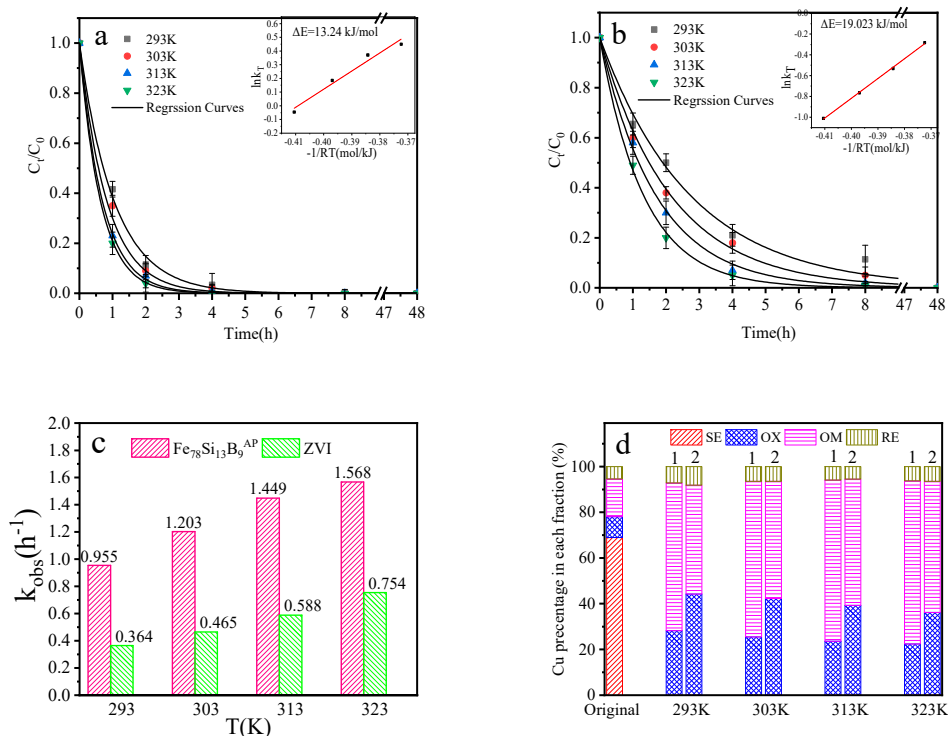

Figure 2. Effect of temperature on the immobilization process of (**a**) $Fe_{78}Si_9B_{13}^{AP}$ and (**b**) ZVI. Insert: The Arrhenius plot of lnk_T versus -1/room temperature (RT) for the remediation of Cu^{2+} ions by (**a**) $Fe_{78}Si_9B_{13}^{AP}$ and (**b**) ZVI. (**c**) Apparent reaction rate. (**d**) Influence of temperature on the fractions of different Cu forms after a 200 h treatment. (1: $Fe_{78}Si_9B_{13}^{AP}$: Treated soils, 2: ZVI: Treated soils).

3.3. The Fractions of Different Cu Forms in Soil after a 200 h Treatment

The existing form of heavy metals in soil is one of the important indicators for an environmental risk assessment. In order to determine the content of each component of the four forms of copper in soil after $Fe_{78}Si_9B_{13}^{AP}$ and ZVI treatment, the method of Ure et al. [32] is used to extract the soil continuously. Figure 2d shows the influence of temperature on the fractions of different Cu forms after a 200 h treatment. The fractions of soluble and exchangeable (SE) in untreated soil is the highest, accounting for 68.94% of the total copper content. The second is the reducible state (OX) accounting for 16.50%. The fractions of oxidizable state (OM) and residual state (RE) is 9.14% and 5.41%, respectively. There is almost no SE in soil after $Fe_{78}Si_9B_{13}^{AP}$ and ZVI treatment. Cu^{2+} is converted to OX and OM by the reduction and adsorption of iron-based materials. The source of OX is the Cu^{2+} combined with iron oxide with high surface energy and low coordination number [41]. The fractions of OX_1 in soil treated with $Fe_{78}Si_9B_{13}^{AP}$ at different temperatures is 28.23%, 25.52%, 23.54%, and 22.36%, respectively. The fractions of OX_2 in the soil after ZVI treatment at different temperatures is 44.24%, 42.25%, 39.24%, and 36.20%, respectively. It can be seen that the fractions of OX_2 are significantly higher than that of OX_1 at all temperatures. This is due to the fact that the particle size of ZVI is much smaller than that of $Fe_{78}Si_9B_{13}^{AP}$, which provides more active sites for the adsorption reaction and is more conducive to the binding of Cu^{2+} ions. Since the extraction of OM is carried out in acidic H_2O_2, this process can not only oxidize the organic matter, but also reoxidize the reduced Cu^0 to Cu^{2+} ions. Therefore, OM includes organically bound copper and elemental copper. The fractions of OM_1 in the soil after $Fe_{78}Si_9B_{13}^{AP}$ treatment is 64.62%, 68.04%, 70.59%, and 71.37%, respectively. The fractions of OM_2 in soil treated with ZVI is 47.62%, 51.26%, 55.27%, and 57.34%, respectively. With the increase in temperature, the fractions of OM_1

and OM_2 show an upward trend, and the values of each group of OM_1 are higher than OM_2. Since the organic bound state does not participate in the immobilization process of Cu^{2+}, the increase of OM fraction is caused by the conversion of Cu^{2+} ions to Cu^0. As a result, the ability of $Fe_{78}Si_9B_{13}{}^{AP}$ to reduce Cu^{2+} ions is higher than that of ZVI. Once the Cu^{2+} ions are reduced to Cu^0, they cannot be dissolved even if they are leached by acid rain for a long time. Combined with the change of OX fraction, it can be determined that the process of immobilization and remediation of copper contaminated soil by two kinds of iron-based materials is mainly the reduction and adsorption reaction, and the increase in temperature is beneficial to the reduction and immobilization. The fraction of RE in the soil is about 6% before and after the treatment. This is due to the fact that the process of replacing silicon, aluminum, and other atoms in the soil lattice by copper is too slow to occur in this experiment.

3.4. Reaction Mechanism Analysis

According to the previous kinetic analysis, it is known that the reduction of Cu^{2+} ions by $Fe_{78}Si_9B_{13}{}^{AP}$ and ZVI is controlled by the diffusion process. Therefore, the morphology and phase of the surface products directly affect the movement of Cu^{2+} ions to the reaction interface. The morphology and phase composition of the surface products before and after the reaction are analyzed by SEM and XRD. Figure 3a shows the morphology of the product on the surface of $Fe_{78}Si_9B_{13}{}^{AP}$. The originally smooth surface is seriously corroded and the product layer on the surface is thin. In order to observe the morphology of the product more clearly, the B region is magnified and displayed in Figure 3b. The product layer presents a three-dimensional flower-like structure composed of nano-lamellar intercalation perpendicular to the reaction interface, and the interstitial pores provide a channel for the diffusion of Cu^{2+} ions to the reaction interface. Figure 3c observed that ZVI is completely surrounded by a dense product layer. Some of the products fall off from the matrix, which is difficult to extract in the later magnetic separation process. Figure 3d shows a high-resolution image of the product layer overlaid on the ZVI. The morphology of the product is dendritic and grows randomly in all directions, which hinders the contact between Cu^{2+} ions and ZVI, which is the main reason for the low activity of ZVI. With regard to the explanation that the morphology of the products of amorphous and crystalline alloys affects the reaction rate, some scholars think that there is an active "liquid-like" layer on the surface of the amorphous alloy [42]. Figure 4 shows a Bragg peak of Cu^0 in the XRD pattern of soil treated with $Fe_{78}Si_9B_{13}{}^{AP}$ and ZVI. The products of Cu^{2+} ions reduction by two kinds of iron-based alloys are Cu^0. Since the standard electrode potential of copper $E(Cu/Cu^{2+})$ is higher than the standard electrode potential of hydrogen $E(H_2/H^+)$, even long-term acid rain leaching cannot dissolve Cu^0 again, effectively reducing the potential risk of copper in the soil.

3.5. Magnetic Separation

The above experimental results show that $Fe_{78}Si_9B_{13}{}^{AP}$ and ZVI can effectively reduce the potential risk of copper in the soil. However, when conditions such as soil pH change, the immobilized copper (such as OX) has the possibility of a secondary release. In addition, iron-based alloys added to the soil will have adverse effects on plant growth and microbial community [43]. In this study, the magnetic separation process is used to recover the stabilizer particles with immobilized products attached to the surface. The extraction result is shown in Figure 5. Since the iron content of ZVI is higher than that of $Fe_{78}Si_9B_{13}{}^{AP}$, the recovery rate of ZVI is relatively high, reaching 68.85%. The recovery rate of $Fe_{78}Si_9B_{13}{}^{AP}$ is slightly lower, only 47.23%. After magnetic separation, the contents of $Fe_{78}Si_9B_{13}{}^{AP}$ and ZVI in soil are 26.36 and 17.07 g/kg, respectively, which are less than the upper limit value. It can be seen that the remediation process does not cause a secondary pollution to the soil. Figure 5b shows that the recovery of copper is not satisfactory. The recovery rate of copper in the soil treated by $Fe_{78}Si_9B_{13}{}^{AP}$ is 21.56%, and the remaining total copper content is 470.64 mg/kg. The recovery rate of copper in the soil treated by ZVI is 32.42%, and the

remaining total copper content is 405.48 mg/kg. It is found that the recovery rate of copper in ZVI treated soil is higher than that of $Fe_{78}Si_9B_{13}{}^{AP}$, which could be explained by the SEM image in Figure 3. The products of ZVI and Cu^{2+} ions are attached to the surface of ZVI, while the adhesion amount of $Fe_{78}Si_9B_{13}{}^{AP}$ surface products is less. Since Cu^0 is not ferromagnetic, copper attached to the surface of the Fe-based alloy can only be extracted in the process of magnetic separation. Therefore, the recovery rate of copper in the soil treated with $Fe_{78}Si_9B_{13}{}^{AP}$ is low. It can be seen from Figure 2d that when the temperature is 323 K, the content of OX and Cu^0 in the soil after the $Fe_{78}Si_9B_{13}{}^{AP}$ treatment is 22.36% and 54.87%, respectively. Under ideal conditions, the recovery rate of copper can reach 77.23%, while the experimental value only reaches 42.23%, the difference between the two is 35%. This is due to the shedding of the product layer and the adsorption of copper by the soil. In order to solve the problem of low magnetic separation rate of copper, the combination of strengthening loose products and stabilizers is being considered in the follow-up experiments.
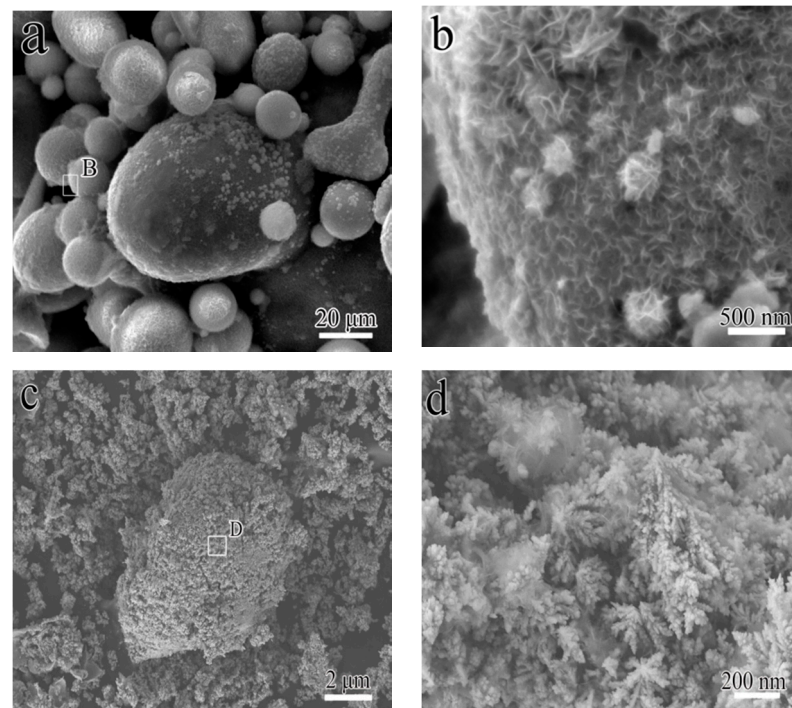

Figure 3. Morphology of the products after the reaction of three materials with Cu^{2+} ions: (**a**) $Fe_{78}Si_9B_{13}{}^{AP}$; (**b**) high resolution image of regional (B); (**c**) ZVI; (**d**) high resolution image of regional (D).
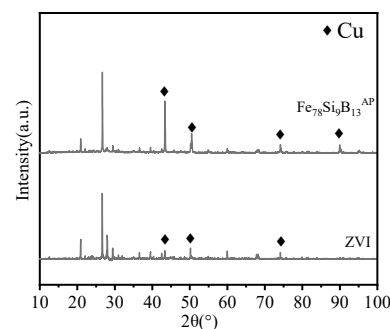

Figure 4. XRD spectra of $Fe_{78}Si_9B_{13}{}^{AP}$ and ZVI after reacting with Cu^{2+} ions.

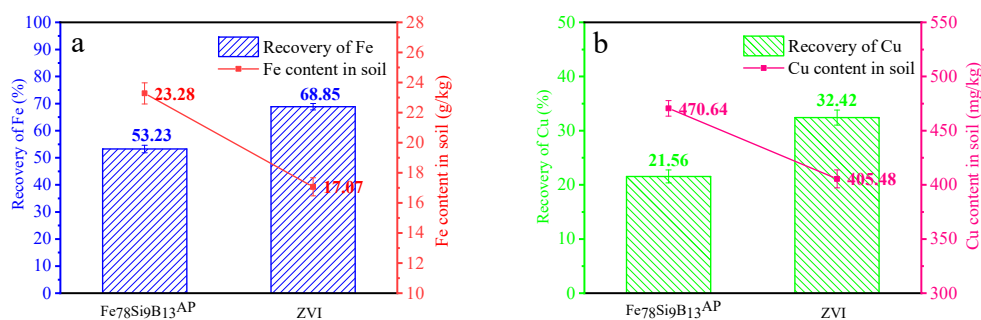**Figure 5.** The recovery of Fe (**a**) and Cu (**b**) from soil by magnetic separation after $Fe_{78}Si_9B_{13}^{AP}$ and ZVI treatment (initial Cu in soil = 600 mg/kg, soil/solution = 1 g/10 mL, stabilizers dosage = 50 g/kg, T = 323 K).

4. Conclusions

In this paper, ZVI is used to compare and analyze the immobilization remediation effect of $Fe_{78}Si_9B_{13}^{AP}$ on copper contaminated soil. The kinetic process of conversion of movable Cu to immobilized forms in the soil system is studied. The feasibility of the magnetic separation process for removing immobilized copper from the soil is verified. The main results and conclusions are summarized as follows:

Compared with the traditional stabilizer ZVI, $Fe_{78}Si_9B_{13}^{AP}$ with a larger particle size and lower iron content can reduce movable copper in the soil more efficiently. According to the fitting analysis of the Arrhenius-type equation, the apparent activation energy of the reaction of $Fe_{78}Si_9B_{13}^{AP}$ and ZVI with Cu^{2+} is 13.24 and 19.02 kJ/mol, respectively, which is controlled by the diffusion process.

The main forms of copper in the immobilized soil are OX and OM. There is almost no SE in the immobilized soil. The bioavailability of copper in the soil is effectively reduced.

The difference in the atomic arrangement between $Fe_{78}Si_9B_{13}^{AP}$ and ZVI results in a great difference in the structure of the product layer. The surface products of $Fe_{78}Si_9B_{13}^{AP}$ have a nano-pore structure, which provides a channel for the movement of Cu^{2+} to the reaction interface. However, ZVI is wrapped in a dense product layer, which hinders the sustainable progress of the reaction.

The recoveries of $Fe_{78}Si_9B_{13}^{AP}$ and ZVI by the magnetic separation process are 47.23% and 68.85%, respectively, and the recoveries of copper in soil treated by $Fe_{78}Si_9B_{13}^{AP}$ and ZVI are 21.56% and 32.42%, respectively. The content of iron and copper in soil is reduced to a certain extent, which has a certain engineering application value.

At present, the production technology of the amorphous alloy is quite mature, and the market price is close to that of micron ZVI, which has the basic conditions for an engineering application. The above research results show that the Fe-based amorphous alloy has a high activity in the treatment of copper-contaminated soil, which solves the problem of low treatment efficiency and material waste caused by ZVI passivation. The purpose of this paper is to provide some inspiration for the application of derived amorphous alloys to the field of soil remediation.

Author Contributions: Conceptualization, L.P. and X.Z.; methodology, L.P.; software, L.P.; validation, L.P., Z.Y. and X.Z.; formal analysis, L.P.; investigation, L.P.; resources, X.Z.; data curation, Z.Y.; writing—original draft preparation, L.P.; writing—review and editing, X.Z.; visualization, L.P.; supervision, Z.Y.; project administration, Z.Y.; funding acquisition, Z.Y. All authors have read and agreed to the published version of the manuscript.

Data Availability Statement: No new data were created or analyzed in this study. Data sharing is not applicable to this article.

Conflicts of Interest: The authors declare no conflict of interest. The funders had no role in the design of the study; in the collection, analyses, or interpretation of data; in the writing of the manuscript, or in the decision to publish the results.

References

1. Baryla, A.; Laborde, C.; Montillet, J.L.; Triantaphylidès, C.; Chagvardieff, P. Evaluation of Lipid Peroxidation as a Toxicity Bioassay for Plants Exposed to Copper. *Environ. Pollut.* **2000**, *109*, 131–135. [CrossRef]
2. Roy, D.N.; Mandal, S.; Sen, G.; Biswas, T. Superoxide Anion Mediated Mitochondrial Dysfunction Leads to Hepatocyte Apoptosis Preferentially in the Periportal Region during Copper Toxicity in Rats. *Chem. Biol. Interac.* **2009**, *182*, 136–147. [CrossRef]
3. Choudhary, M.; Jerley, U.K.; Abash Khan, M.; Zutshi, S.; Fatma, T. Effect of Heavy Metal Stress on Proline, Malondialdehyde, and Superoxide Dismutase Activity in the Cyanobacterium Spirulina platensis-S5. *Ecotox. Environ. Safe.* **2007**, *66*, 204–209. [CrossRef] [PubMed]
4. Attaeian, B.; Mortazavi, S.; Farokhzadeh, B.; Khorsand, M. Evaluation and Mapping Spatial Distribution of Copper Pollution in Soil and Water of Vineyard Garden. *J. Environ. Health Sci.* **2019**, *6*, 293–310. [CrossRef]
5. Parada, J.; Rubilar, O.; Diez, M.C.; Cea, M.; Sant'Ana da Silva, A.; Rodríguez-Rodríguez, C.; Tortella, G.R. Combined pollution of copper nanoparticles and atrazine in soil: Effects on dissipation of the pesticide and on microbiological community profiles. *J. Hazard. Mater.* **2019**, *361*, 228–236. [CrossRef]
6. Georgieva, V.G.; Gonsalvesh, L.; Tavlieva, M.P. Thermodynamics and kinetics of the removal of nickel (II) ions from aqueous solutions by biochar adsorbent made from agro-waste walnut shells. *J. Mol. Liq.* **2020**, *312*, 112788. [CrossRef]
7. Islam, A.; Awual, R.; Angove, M.J. A review on nickel(II) adsorption in single and binary component systems and future path. *J. Environ. Chem. Eng.* **2019**, *7*, 103305. [CrossRef]
8. Zhu, Y.; Fan, W.; Zhou, T.; Li, X. Removal of chelated heavy metals from aqueous solution: A review of current methods and mechanisms. *Sci. Total Environ.* **2019**, *678*, 253–266. [CrossRef]
9. Gong, Y.; Zhao, D.; Wang, Q. An overview of field-scale studies on remediation of soil contaminated with heavy metals and metalloids: Technical progress over the last decade. *Water Res.* **2018**, *147*, 440–460. [CrossRef] [PubMed]
10. Zhang, H.; Shao, J.; Zhang, S.; Zhang, X.; Chen, H. Effect of Phosphorus-Modified Biochars on Immobilization of Cu (II), Cd (II), and As (V) in Paddy Soil. *J. Hazard. Mater.* **2019**, *390*, 121349. [CrossRef] [PubMed]
11. Viglašová, E.; Dano, M.; Galambos, M.; Krajnak, A. Investigation of Cu(II) adsorption on Slovak bentonites and illite/smectite for agricultural applications. *J. Radioanal. Nucl. Chem.* **2017**, *314*, 2425–2435. [CrossRef]
12. Cui, H.; Zhang, X.; Wu, Q.; Zhang, S.; Xu, L.; Zhou, J.; Zhang, X.; Zhou, J. Hematite enhances the immobilization of copper, cadmium and phosphorus in soil amended with hydroxyapatite under flooded conditions. *Sci. Total Environ.* **2020**, *708*, 134590. [CrossRef]
13. Stefania, B.; Paolo, S.C.; Nicola, O. Critical aspects related to Fe0 and Fe0/pumice PRB design. In *Coupled Phenomena in Environmental Geotechnics*; CRC Press: Boca Raton, FL, USA, 2013.
14. Moraci, N.; Ielo, D.; Bilardi, S.; Calabrò, P.S. Modelling long-term hydraulic conductivity behaviour of zero valent iron column tests for permeable reactive barrier design. *Can. Geotech. J.* **2016**, *53*, 946–961. [CrossRef]
15. Cao, M.; Tu, S.; Xiong, S.; Zhou, H.; Chen, J.; Lu, X. EDDS enhanced PCB degradation and heavy metals stabilization in co-contaminated soils by ZVI under aerobic condition. *J. Hazard. Mater.* **2018**, *358*, 265–272. [CrossRef] [PubMed]
16. Liu, Y.; Wang, J. Reduction of nitrate by zero valent iron (ZVI)-based materials: A review. *Sci. Total Environ.* **2019**, *671*, 388–403. [CrossRef] [PubMed]
17. Zhao, X.; Liu, W.; Cai, Z.; Han, B.; Qian, T.; Zhao, D. An overview of preparation and applications of stabilized zero-valent iron nanoparticles for soil and groundwater remediation. *Water Res.* **2016**, *100*, 245–266. [CrossRef]
18. Frick, H.; Tardif, S.; Kandeler, E.; Holm, P.E.; Brandt, K.K. Assessment of biochar and zero-valent iron for in-situ remediation of chromated copper arsenate contaminated soil. *Sci. Total Environ.* **2019**, *655*, 414–422. [CrossRef]
19. Kumpiene, J.; Ore, S.; Renella, G.; Mench, M.; Lagerkvist, A.; Maurice, C. Assessment of zerovalent iron for stabilization of chromium, copper, and arsenic in soil. *Environ. Pollut.* **2006**, *144*, 62–69. [CrossRef] [PubMed]
20. Sriram, G.; Kigga, M.; Uthappa, U.T.; Rego, R.M.; Thendral, V.; Kumeria, T.; Jung, H.; Kurkuri, M.D. Naturally available diatomite and their surface modification for the removal of hazardous dye and metal ions: A review. *Adv. Colloid Interface* **2020**, *282*, 102198. [CrossRef]
21. Molnár, Á. Catalytic applications of amorphous alloys: Expectations, achievements, and disappointments. *Appl. Surf. Sci.* **2010**, *257*, 8151–8164. [CrossRef]
22. Azuma, D.; Ito, N.; Ohta, M. Recent progress in Fe-based amorphous and nanocrystalline soft magnetic materials. *J. Magn. Magn. Mater.* **2020**, *501*, 166373. [CrossRef]
23. Zhang, C.; Zhang, H.; Lv, M.; Hu, Z. Decolorization of azo dye solution by Fe-Mo-Si-B amorphous alloy. *J Non-Cryst. Solids* **2010**, *356*, 1703–1706. [CrossRef]

24. Zhang, X.; Liu, J.; Li, J.; Li, C.; Yuan, Z. Excellent capability in remediating Cu^{2+} from aqueous solution by Fe-Si-B amorphous alloys. *Appl. Phys. A* **2020**, *126*, 219. [CrossRef]

25. Liang, S.X.; Zhang, W.; Zhang, L.; Wang, W.; Zhang, L.C. Remediation of industrial contaminated water with arsenic and nitrate by mass-produced Fe-based metallic glass: Toward potential industrial applications. *Sustain. Mater. Technol.* **2019**, *22*, 00126. [CrossRef]

26. Cao, C.R.; Lu, Y.M.; Bai, H.Y.; Wang, W.H. High surface mobility and fast surface enhanced crystallization of metallic glass. *Appl. Phys. Lett.* **2015**, *107*, 577. [CrossRef]

27. Chen, F.; Lam, C.H.; Tsui, O.K.C. The Surface Mobility of Glasses. *Science* **2014**, *343*, 975–976. [CrossRef] [PubMed]

28. Soil Environmental Quality Risk Control Standard for Soil Contamination of Development Land GB36600-2018. Available online: http://www.mee.gov.cn/ywgz/fgbz/bz/bzwb/trhj/201807/t20180703_446027.shtml (accessed on 20 September 2020).

29. Zhao, B.W.; Wang, G. Preliminary InVestigation and Assessment of Farmland Soils Contaminated by Heavy Metal around Baiyin City. *Environ. Sci. Tech.* **2010**, *33*, 79–81.

30. Shaaban, M.; Wu, Y.; Peng, Q.; Wu, L.; Zwiseten, L.V.; Khalid, M.S.; Younas, A.; Lin, S.; Bashir, S. The interactive effects of dolomite application and straw incorporation on soil N_2O emissions: Nitrous oxide emissions from an acidic soil. *Eur. J. Soil Sci.* **2018**, *69*, 505–511. [CrossRef]

31. Ji, Z.H.; Pei, Y.S. Immobilization efficiency and mechanism of metal cations (Cd^{2+}, Pb^{2+} and Zn^{2+}) and anions ($AsO4^{3-}$ and $Cr2O7^{2-}$) in wastes-based geopolymer. *J. Hazard. Mater.* **2020**, *384*, 121290. [CrossRef]

32. Kumpiene, J.; Lagerkvist, A.; Maurice, C. Stabilization of As, Cr, Cu, Pb and Zn in soil using amendments—A review. *Waste Manag.* **2008**, *28*, 215–225. [CrossRef]

33. Ure, A.M.; Quevauviller, P.; Muntau, H.; Griepink, B. Speciation of heavy metals in soils and sediments. An account of the improvement and harmonization of extraction techniques undertaken under the auspices of the BCR of the commission of the european communities. *Int. J. Environ. An. Ch.* **1993**, *51*, 135–151. [CrossRef]

34. Guan, X.; Yang, H.; Sun, Y.; Qiao, J. Enhanced immobilization of chromium(VI) in soil using sulfidated zero-valent iron. *Chemosphere* **2019**, *228*, 370–376. [CrossRef]

35. Mijatovi, N.; Terzi, A.; Milii, L.; Lvojinovi, D. Immobilization of heavy metal ions Zn^{2+}, Ni^{2+}, Pb^{2+} and Cu^{2+} in the structure of cement-based materials. *Zastita Materijala* **2020**, *61*, 116–127. [CrossRef]

36. Mohan, V.B.; Jayaraman, K.; Bhattacharyya, D. Brunauer–Emmett–Teller (BET) specific surface area analysis of different graphene materials: A comparison to their structural regularity and electrical properties. *Solid State Commu.* **2020**, *320*, 114004. [CrossRef]

37. Wang, P.; Wang, J.Q.; Li, H.; Yang, H.; Huo, J.; Chang, C.; Wang, X.; Li, R.W.; Wang, G. Fast decolorization of azo dyes in both alkaline and acidic solutions by Al-based metallic glasses. *J. Alloys Compd.* **2017**, *701*, 759–767. [CrossRef]

38. Tong, X.; Wang, G.; Stachurski, Z.H.; Bednarčík, J.; Mattern, N.; Zhai, Q.J.; Eckert, J. Structural evolution and strength change of a metallic glass at different temperatures. *Sci. Rep-UK* **2016**, *6*, 386–474. [CrossRef]

39. Chen, J.; Zhu, L. Heterogeneous UV-Fenton catalytic degradation of dyestuff in water with hydroxyl-Fe pillared bentonite. *Catal. Today* **2007**, *126*, 463–470. [CrossRef]

40. Lien, H.L.; Zhang, W.X. Nanoscale Pd/Fe bimetallic particles: Catalytic effects of palladium on hydrodechlorination. *Appl. Catal. B-Environ.* **2007**, *77*, 110–116. [CrossRef]

41. Phuengprasop, T.; Sittiwong, J.; Unob, F. Removal of heavy metal ions by iron oxide coated sewage sludge. *J. Hazard. Mater.* **2011**, *186*, 502–507. [CrossRef]

42. Cao, C.R.; Huang, K.Q.; Shi, J.A.; Zheng, D.N.; Wang, W.H.; Gu, L.; Bai, H.Y. Liquid-like behaviours of metallic glassy nanoparticles at room temperature. *Nat. Commun.* **2019**, *10*, 1–8. [CrossRef]

43. Su, H.; Fang, Z.; Tsang, P.E.; Zheng, L.; Zhao, D. Remediation of hexavalent chromium contaminated soil by biochar-supported zero-valent iron nanoparticles. *J. Hazard. Mater.* **2016**, *318*, 533–540. [CrossRef] [PubMed]